ELSEVIER

Surface Science 425 (1999) 259–275

surface science

An investigation of the surface reaction mechanisms of alternating-grown, ordered atomic layers: CdS on ZnSe(100)

M. Han, Y. Luo, J.E. Moryl, R.M. Osgood Jr. *

Columbia Radiation Laboratory, Columbia University, New York, NY 10027, USA

Received 5 October 1998; accepted for publication 11 January 1999

Abstract

Temperature-programmed desorption (TPD) is used for detailed investigation of the surface chemistry of a binary reaction sequence by sequential gas-phase dosing of a ZnSe(100) substrate with $(CH_3)_2Cd$ and H_2S. Analysis of the TPD spectra shows that adsorbed DMCd irreversibly dissociates on a ZnSe(100)-c(2×2) surface at room temperature to form a fully methyl-terminated surface; this termination is responsible for the previously reported, self-limiting reaction. At ~370 K, DMZn desorbs from this surface due to a methyl-exchange reaction. This desorption temperature is independent of coverage, indicating a first-order reaction. In addition, at high DMCd exposures, the adsorption/desorption process leads to replacement of surface Zn by Cd. The experiments also examine the reaction of H_2S with the methyl-terminated surface. This reaction, which is also self-limiting, forms a sulfur-hydride-terminated surface after the release of surface CH_3 groups in the form of CH_4.

Studies of surfaces formed by more than one binary reaction sequence are also reported, which show that the alternating growth surfaces are terminated with either methyl groups or hydrogen. The methyl-passivated growth surface preferentially desorbs methyl radicals at ~390 K instead of the metal-alkyl species. For the sulfur-hydride-terminated surface the recombinative reaction of the HS species causes desorption of H_2S at 480 K. In this case, the symmetric peak shape of the desorbed H_2S signal and its shift to lower temperature with increasing the coverage suggest a second-order reaction mechanism. In more general terms, these results indicate that the relative strengths of bond for methyl–metal (II) and metal–VI element play an important role in the surface reactions.

Keywords: Temperature-programmed desorption (TPD); Atomic layer epitaxy (ALE); Near edge X-ray absorption fine structure (NEXAFS); Surface reaction; Organometallic chemistry; $(CH_3)_2Cd$; $(CH_3)_2Zn$; H_2S; Thin film deposition; II–IV semiconductors; CdS; ZnSe(100)

1. Introduction

Organometallic surface reactions are fundamental to many applications in thin-film growth and synthetic chemistry. As a result there is an extensive literature on their reaction mechanisms and pathways. More recently, however, there has been an increasing interest in examining the application of such reactions to form an ordered array of chemisorbed atoms and, in some cases, to use a sequence of such reactions to realize either lateral and vertical ordering. One of the most striking examples of such a reaction sequence has been in the growth of epitaxial layers of semiconducting materials as well as in the closely related problem of designed semiconducting interfaces. The interest in the former, sometimes called atomic layer epi-

* Corresponding author. Fax: +1 212 8541909.
E-mail address: osgood@columbia.edu (R.M. Osgood)

0039-6028/99/$ – see front matter
PII: S0039-6028(99)00198-3

taxy (ALE), is motivated by the need for control of layer thickness and uniformity [1–5].

Ideally, ALE achieves monolayer-scale growth control through alternation of a set of reactive molecular precursors, with each reaction step exhibiting saturation of the chemisorbed monolayer due to one or more surface phenomena, e.g. layer-dependent reaction activation, site blocking, etc. For example, the presence of stable surface ligands from the molecular precursor after each growth step will limit further reaction of the precursor [4–6]. Note also that surface ligands can help stabilize a full monolayer of the deposited element [1,7]. Unlike many applications of organometallic chemistry, ALE requires that the products be inserted into specific, ordered reaction sites. Typically such ordering is achieved thermodynamically with the aid of thermally activated surface migration, although it should also be possible to have the chemisorption step directly deposit an atom in its desired lattice position as a result of very site-selective reactions on an initially ordered growth surface. The intent of this and other recent related work is to investigate the use of self-limiting organometallic surface reactions to achieve ordered growth through the latter mechanism. In this latter form of atomic layer epitaxy, i.e. that resulting from a surface-chemical-reaction-driven process, ordered growth is achieved by a sequence of two surface reactions involving insertion of a lattice constituent in place of a thermally stable surface ligand. A complete understanding of such a process must thus address the detailed chemistry controlling adsorption or reaction of precursors on both substrate and grown surfaces, and their adsorbed intermediates.

For example, previous studies in our laboratory [8,9] have shown that atomic layer epitaxy of CdS on ZnSe(100), a model system for II–VI heteroepitaxy, can be achieved at room temperature using a binary reaction sequence, which consists in alternately dosing two molecular precursors, dimethylcadmium (DMCd) and hydrogen sulfide (H_2S), onto a ZnSe(100) substrate. Our studies of organometallic and hydride reactions on semiconductor surfaces have shown that these molecular species exhibit considerable surface selectivity which is important in the ALE process. For example, the molecular precursor H_2S does not chemisorb on a well-prepared, Zn-rich ZnSe(100)-c(2×2) surface at room temperature, while it reacts strongly with the Ga-rich surface of GaAs(100) [10,11]. On the other hand, our ALE process is initiated by facile chemisorption of DMCd on this same ZnSe(100)-c(2×2) surface. Our TPD results, which are described here, show that DMCd dissociates on ZnSe(100)-c(2×2) substrate and forms a methyl-terminated surface. This finding appears to be different than that of Vohs and Sides [2,12] who reported that DEZn and DMCd adsorb reversibly and apparently intact on II–VI semiconductor surface, i.e. as grown ZnSe(100) and the CdTe(100)-c(2×2) surfaces respectively.

In our model II–VI system, the self-limiting reaction in each step of the reaction sequence results in layer-by-layer growth. This process was first studied using in situ AES, XPS, and LEIS probes of the growth surface after each step in the sequence [8,9]. The growth was initiated on ZnSe(100)-c(2×2) which is the stable surface structure for several II–VI (100) surfaces when terminated by the group II metal [13,14]. LEED measurements of the grown surface have been reported in previous papers [8,9]. The results showed that, while the surface order decreased somewhat in the initial growth stages, a highly ordered thin film was observed after deposition of more than 6–7 bilayers of CdS. In addition, more recently, an investigation using near edge X-ray adsorption fine structure (NEXAFS) spectroscopy [15] showed that, at room temperature, the growth surfaces were alternatively passivated by methyl or sulfur-hydride ligands, thus preventing further uptake of Cd or S, respectively. These results are in accord with the sketch of the binary surface reaction sequence as shown in Fig. 1.

In this paper, we study the surface reaction mechanisms during both the initial and subsequent growth stages using temperature-programmed desorption (TPD). First, thermal desorption studies are made to determine the surface species, including both ligands and crystal constituents, after a saturated monolayer is formed by reaction with either DMCd or H_2S. The desorption process generally, but not exclusively, results in ligand-

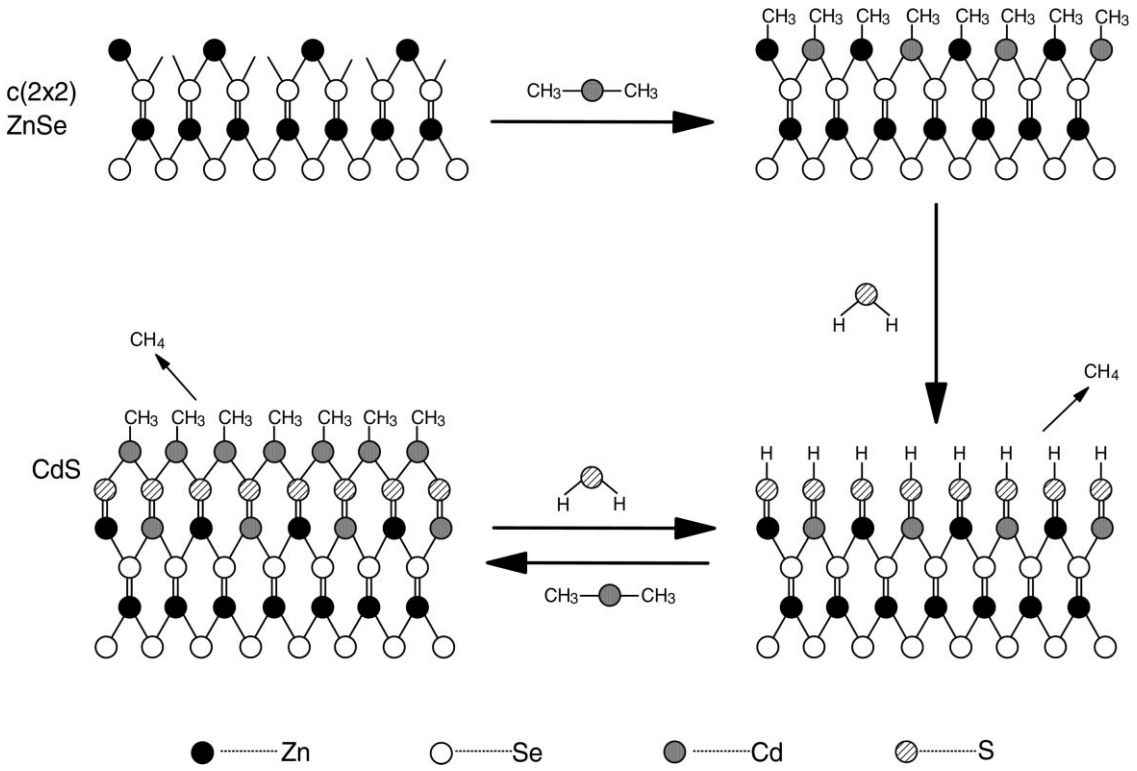

Fig. 1. Schematic representation of the ordered bilayer growth examined in this work. Layer by layer growth is achieved by the repetition of two chemisorption reactions. Note that a different reaction for the initial step on the ZnSe(100)-c(2×2) substrate.

aided abstraction of Group II or VI atoms from the crystal surface layer. Second, a more detailed study is then made of the chemisorption reactions for the first bilayer. In this case, the dependence of the concentration of surface products on DMCd exposure is made for surfaces with both half and integral numbers of bilayers. These experiments enable an investigation to be made of the importance of metal migration in the top few layers during the growth process as well as the trade-off between metal abstraction and deposition during growth.

2. Experimental

The experiments were carried out in an ultra-high vacuum (UHV) chamber equipped with a differentially pumped quadrupole mass spectrometer for TPD, a hemispherical energy analyzer for Auger electron spectroscopy (AES), a low energy electron diffraction (LEED) system, and an ion gun for low energy ion scattering (LEIS) and sputter cleaning the sample. The chamber had a base pressure of 5.0×10^{-11} mbar, which was achieved by a 550 l s^{-1} turbomolecular pump and a titanium sublimation pump.

The preparation of the ZnSe(100) substrate has previously been described in detail [8,9]. Briefly, a chemically polished ZnSe substrate (II–VI, Inc.) with dimensions $1\times1\times0.1$ cm was indium bonded onto a molybdenum foil. The temperature of the resistively heated or liquid-nitrogen-cooled substrate was measured with a K-type chromel–alumel thermocouple spot welded to the back of the molybdenum foil. The surface was sputtered at room temperature with 1000 eV Ar^+ followed by annealing at 425°C for 15 min and 435°C for 3 min. The preparation of a clean, ordered ZnSe(100)-c(2×2) surface [13,14] was verified

with AES and LEED. The precursors, DMCd (Strem Chemical, 99.999%) and H_2S (Matheson, 99.5%) were purified by repetitive freeze–pump–thaw cycles and introduced to the growth surface via two separate dosing tubes located close to the surface. The flux of each of the precursors on the sample was controlled by a leak valve and monitored by measuring the pressure rise in the dosing chamber. In this paper, exposure data are given in terms of a relative exposure scale. This relative exposure was obtained by multiplying the overall chamber pressure (constant during dosing) by the dosing time. An approximate calibration of the actual exposure level of the sample surface was obtained by first static backfilling of the chamber and then cross checking the amount of adsorbed species, using TPD, with that obtained with the dosing apparatus. This experiment showed that the actual exposure obtained using the dosing apparatus is approximately 3×10^3 times higher than that calculated based on the overall chamber pressure.

The mass spectrometer was enclosed in a water-cooled shroud with a 3 mm diameter aperture located in front of the ionizer. The sample was positioned within 1 mm of this aperture during TPD experiments to allow species desorbing from the surface to be preferentially admitted to the mass spectrometer. This procedure was found to minimize or eliminate desorption signals from other parts of the substrate holder. A heating rate of $4\ \mathrm{K\ s^{-1}}$ was used in all of the TPD measurements. Computer multiplexing allowed the temperature to be sampled and the heating rate to be controlled. As many as twelve separate mass-to-charge ratios could be monitored simultaneously. Desorption products were assigned by comparison with mass spectrometer cracking patterns obtained both from the literature and from measurements taken in our laboratory under the same conditions as those during TPD. For our mass spectrometer, the relative CH_3/CH_4 signal was always observed to be ~1 in the cracking patterns of the physisorbed molecular DMCd, desorption product of DMZn, methyl radical, and gas-phase methane. Typically, a low, $m/e^+=15$ to 16 intensity ratio of 1:1 is assigned to methane desorption, and an intensity ratio of 4:1 to methyl-radical desorption [16]. In our case, no distinction in the cracking patterns for methyl radicals and methane was observed, probably because of the presence of residual H_2 and other hydrides in the chamber. The existence of an H_2 background was determined by residual gas analysis (RGA) in our chamber and may be attributed to the presence of H_2S, which was introduced as a reactant.

3. Results

3.1. TPD spectra from adsorbed or grown surfaces

This section discusses the surface adsorbates formed, after saturated exposure to one of the two molecular precursors, DMCd and H_2S. As mentioned in the introduction, experiments with Auger and NEXAFS spectroscopies, reported in Refs. [8,15], had earlier shown that, after each half-cycle of exposure to one of these precursors, the surface composition changed in cyclic manner from the cation to the anion species, and that after each full cycle a chemisorbed bilayer, i.e. a single layer of CdS, was formed. This same work also suggested that the surface ligands were methyl groups for the cation termination and hydrogen for the anion termination.

3.1.1. Methyl-terminated surfaces

The first series of experiments examined a surface prepared as a result of saturated chemisorption of DMCd on bare ZnSe(100)-c(2×2) to form 0.5 bilayer, or on a sulfur-hydride-terminated surface to form 1.5, 3.5, etc., bilayers. The most important TPD spectra for the adsorbates and growth products on the DMCd-dosed surfaces are summarized in Figs. 2 and 3, which display the fragments observed at mass-to-charge ratios (m/e^+) of 15, 79, 112, and 127, for specific numbers of chemisorbed bilayers. In both figures, the TPD features change with the number of bilayers of CdS. As will be shown below, after exposure to DMCd the surface was left terminated with methyl groups. In addition to the spectra shown in Figs. 2 and 3, other hydrocarbon fragments ($m/e^+=$ 14, 16, 28, 29, 30) were monitored during the TPD experiment. No desorption peaks for $m/e^+=28$,

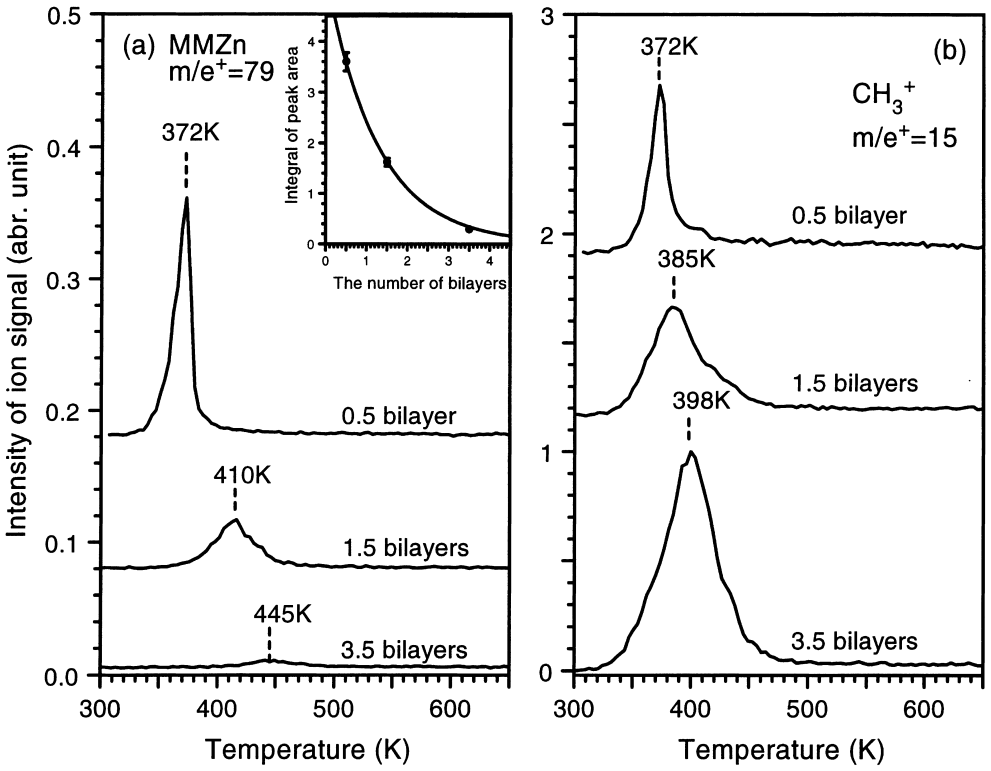

Fig. 2. TPD spectra taken from three different half-bilayer surfaces, i.e. 0.5, 1.5 and 3.5 bilayer surfaces: (a) for $m/e^+ = 79$, monomethyl zinc (MMZn), and (b) for $m/e^+ = 15$, methyl (CH_3). The inset in (a) plots the integrated intensity signal versus the number of bilayers.

29, 30 were observed, suggesting that neither surface dehydrogenation nor recombinative reactions of methyl groups occurred to form desorbed ethylene, free ethyl radicals, or ethane. The TPD spectra for $m/e^+ = 14$ and 16 showed identical behavior to that for $m/e^+ = 15$, thus, indicating that all three peaks originated from the same desorbed species.

Consider first the TPD spectra arising from the desorption of metal and organometallic species. TPD studies of the growth surface for the first few half-bilayers showed, surprisingly, the presence of zinc species even after several growth cycles. For example, Fig. 2a shows the TPD spectra for $m/e^+ = 79$, corresponding to the mass of monomethylzinc (MMZn) from 0.5, 1.5 and 3.5 bilayer surfaces. A sharp, intense feature is observed at about 370 K in the 0.5 bilayer spectrum. For the 1.5 bilayer surface, this peak broadens, with smaller amplitude, and shifts to higher temperature, $\sim$410 K. In the spectrum from the 3.5 bilayer surface, only a weak, broad peak is seen, which is shifted to even higher temperature, $\sim$445 K. Although not shown in Fig. 2, peaks at m/e^+ values characteristic of zinc and dimethylzinc (i.e. $m/e^+ = 64$, 94) were also detected at the same temperatures as for MMZn from these three surfaces. Based on the ratio of the $m/e^+ = 64$, 79 and 94 peaks and the known mass spectrometer cracking pattern for dimethylzinc, these peaks can be attributed to the desorption of this organometallic compound. The MMZn peak was selected as representative of DMZn since the signal of $m/e^+ = 79$ is more intense than that for the parent ion, and, thus, this peak shows clearly the change in the amount of desorbed DMZn.

The inset to Fig. 2a shows the integrated MMZn desorption signal for the three different layer thicknesses shown in the figure. The data demonstrate that, with an increase in the number of the depos-

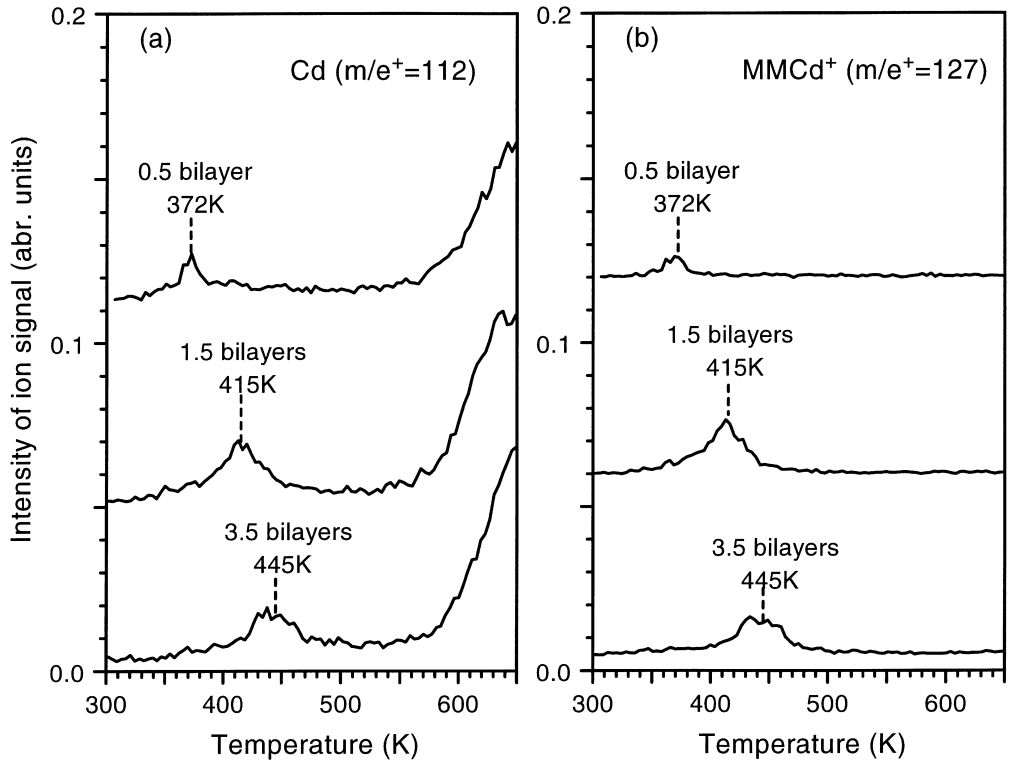

Fig. 3. TPD spectra taken from three different half-bilayer surfaces, i.e. 0.5, 1.5 and 3.5 bilayer surfaces: (a) for mass $m/e^+ = 112$, cadmium (Cd), and (b) for $m/e^+ = 127$, monomethyl cadmium (MMCd).

ited layers, the amount of DMZn desorption decays exponentially. The shift of the TPD peak to higher temperature as the number of bilayers increases reflects the differing surface composition in the top layer. The 0.5 bilayer surface is formed by reaction of the DMCd with the clean substrate to fill in the metal-atom vacancies in the ZnSe(100)-c(2×2) surface and hence surface Zn is copious, i.e. $\sim$0.5 ML in this case. However, zinc appears to be always present in the top metal surface, to at least some extent, with the concentration dependent on the number of CdS bilayers. A more extensive discussion regarding the reaction mechanism for this layer will be presented in Section 3.2.1. Because of its relevance to crystal growth, it would be of interest to know whether Zn diffusion to the surface layer was dominantly the result of migration during the high temperature TPD ramp or alternatively during the growth process itself. Limited experiments were done on this question by varying the maximum temperature of the TPD ramp. These experiments were conducted as follows: first, the surface was dosed with DMCd to saturation at room temperature and the initial TPD was taken, with a maximum ramp temperature of either 430 or 670 K. Note, heating the sample to either of these two temperatures will cause complete desorption of methyl groups in the form of DMZn, and thereby remove the top half-monolayer of Zn atoms. However, the higher temperature would enable greater Zn migration during the temperature ramp, if this process controls the surface Zn concentration. The surface was then dosed a second time with DMCd at room temperature, and a comparison TPD curve was obtained with a temperature ramped to 670 K. Comparing the magnitudes of DMZn desorption signals from different TPD runs provides a probe of the surface Zn concentration under different conditions. For each of the two comparison TPD

runs (i.e. one run for each of the two initial TPD with different final temperatures), identical DMZn desorption peaks were observed at 372 K with a peak intensity $\sim 2/3$ of that obtained in the initial TPD ramp. These results suggest that Zn migration to the surface is not a dominantly thermally driven process, occurring during the TPD, but instead is a more complicated consequence of the growth chemistry.

Fig. 3a and b displays the TPD spectra of Cd and MMCd ($m/e^+ = 112$, 127), respectively, measured on surfaces, after 0.5, 1.5, and 3.5 bilayers have been formed. Although it is not shown in the figure, $m/e^+ = 142$ was also measured. Essentially identical peak profiles and positions were observed for Cd, MMCd, and DMCd. The relative intensities of these three m/e^+ peaks are in good agreement with the DMCd cracking pattern measured with our apparatus under identical instrumental settings, indicating all three of these mass peaks originate from DMCd. As shown in Fig. 3a, in addition to the desorption peak below 500 K, the intensity of $m/e^+ = 112$ signal increased sharply for temperatures above 550 K; this feature originates from sublimation of Cd atoms from the grown layer. The mass signals from desorbed DMCd are small in comparison with those of DMZn from the first layer. Their magnitudes are comparable with that of the DMZn signal from the 3.5 bilayer surface. Additionally, the peak positions for desorption of DMCd change in exactly the same manner as for DMZn on these three surfaces. These results show that the evolution of DMCd is not a dominant desorption pathway on methyl-metal-terminated surfaces even when surface is covered by a full monolayer of Cd, terminated with methyl groups, i.e. 1.5 and 3.5 bilayers. Under these conditions, the surface methyl groups preferentially combine with Zn and desorb as DMZn, if Zn atoms are present. In the absence of significant Zn concentration, as on the 3.5 bilayer surface, most of the methyl groups desorb directly (see discussed below), which implies that Cd bonds more strongly to the subsurface S atoms than to any capping CH_3 group, thus preventing desorption of DMCd.

Returning to the $m/e^+ = 15$ (methyl) features given in Fig. 2b, the spectrum from the first layer shows that the temperature and shape of the peak are the same as those for MMZn as seen in Fig. 2a. Further, the ratio of the peak intensities of CH_3 to MMZn agrees with the cracking pattern of DMZn, indicating in the first layer, all surface methyl groups migrate to surface Zn sites and desorb as DMZn at ~ 370 K (see the sketch in Fig. 4a. Note that no additional hydrocarbon desorption feature was seen with temperatures as high as 700 K for the 0.5 bilayer sample. These results in conjunction with earlier NEXAFS experiments on this same system demonstrate that the 0.5 bilayer surface is covered with adsorbed methyl species.

However, a different behavior was observed in the $m/e^+ = 15$ spectra for the 1.5 and 3.5 bilayer surfaces from that of the first layer. The desorption peak shifts to higher temperatures and broadens with increased layer thickness. In addition, it does not exhibit the same quantitative behavior as the MMZn signal which decreases with the number of bilayers. Specifically, in the spectrum of 1.5 bilayer surface, the mass 15 desorption feature is large and broad, and is centered at 385 K. A more striking result was observed for the 3.5 bilayer surface, namely, this desorption signal is much larger than that from the first layer and is centered at 398 K. Other measurements, see Fig. 3, showed that no significant Cd-alkyl species were produced in this temperature range. Taken together, all these results show that methyl groups desorb predominantly as either free methyl groups (see the sketch in Fig. 4b) or as CH_4 (resulting from a dehydrogenation reaction with a neighboring CH_3 group) when the surface has a low concentration of Zn, i.e. 1.5, 3.5 bilayer surfaces. As indicated above the exception is that trace amounts of surface Zn, resulting from diffusion, cause some surface methyl to desorb as DMZn. However, the amount of DMZn evolution decreases rapidly with the number of deposited layers. The question as to whether the $m/e^+ = 15$ signal originates from desorbed CH_3 or CH_4 is addressed in Section 4 below.

3.1.2. H-terminated surfaces

After chemisorption of DMCd, the surface is left covered with Cd/Zn, terminated by methyl

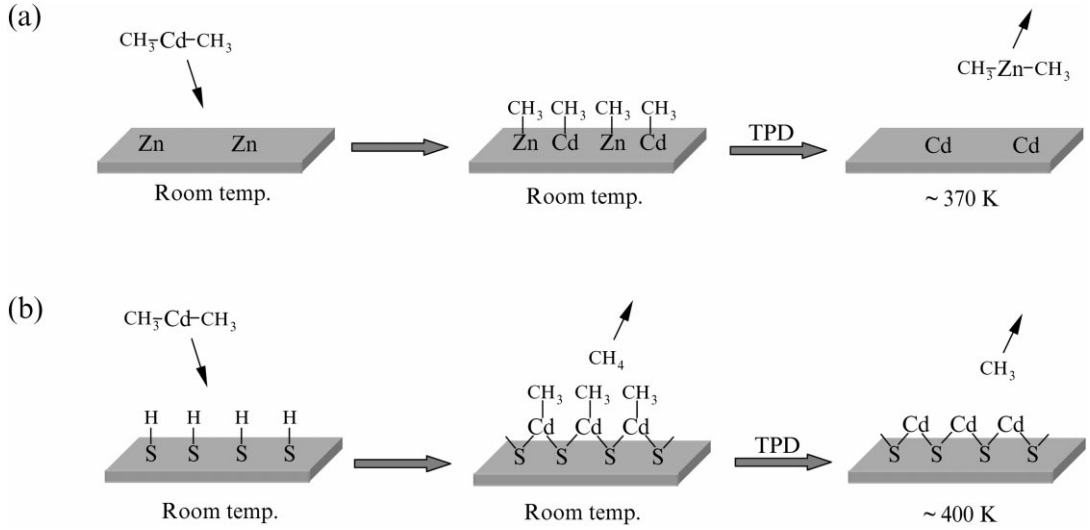

Fig. 4. Schematic depiction of the surface chemistry for methyl-terminated surfaces. Two major TPD pathways are seen: (a) a methyl-exchange reaction following DMCd dosing of a bare ZnSe(100)-(2×2) surface and (b) direct methyl desorption following DMCd dosing of a S–H terminated surface.

ligands. The methyl-terminated surface was then dosed with H_2S to chemisorb sulfur by displacement of methyl ligands. This chemisorption step, shown schematically in Fig. 1, had earlier been verified by NEXAFS measurements. The measurements also suggested that a sulfur-hydride-terminated surface is then formed.

After saturating H_2S exposure, thermal desorption spectra were used to probe several possible products, including Zn, MMZn, DMZn, Cd, MMCd, and DMCd. These species were not detected and, in fact, the only detectable desorption signals were at m/e^+ values corresponding to CH_3 and H_2S. A comparison of the TPD spectra of CH_3 and H_2S, i.e. $m/e^+=15$ and 34, respectively, for the 1.0, 2.0 and 4.0 bilayer surfaces is shown in Fig. 5.

The top three spectra in Fig. 5 show the TPD signals for $m/e^+=15$, methyl radicals. The peak desorption temperatures for these three surfaces were located between ~330 and 430 K, which is the same temperature range for methyl desorption from the 1.5 and 3.5 bilayer surfaces (see Fig. 2b). The methyl coverage for each of the three bilayer samples in Fig. 5 can be estimated by first assuming that the area of $m/e^+=15$ desorption peak from the 3.5 bilayer, methyl-terminated surface, Fig. 2b,

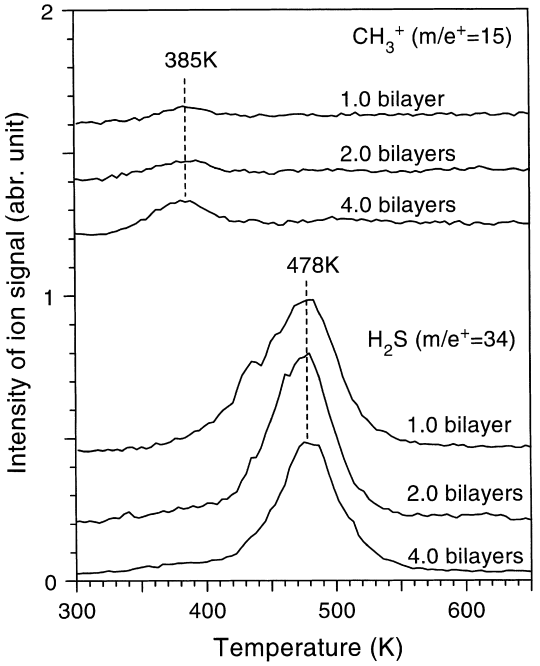

Fig. 5. TPD spectra for CH_3 (top) and H_2S (bottom) taken from three different full-bilayer surfaces, i.e. 1.0, 2.0 and 4.0 bilayer surfaces.

can be taken as the value for the desorbed signal from one monolayer of methyl groups. Then measurement of the integrated $m/e^+ = 15$ signal from the 1.0, 2.0 and 4.0 bilayer surfaces and normalization of these signals with that from the 3.5 bilayer sample, give a methyl coverage of about 4%, 5% and 10% of a monolayer, respectively, for the three surfaces in Fig. 5. Finally, additional experiments showed that these CH_3 signals were independent of the total H_2S exposure, but generally correlated with the DMCd exposure used in preparing the bilayer. As a result, we attribute these features to the exposure of trace amount of DMCd gas which remains in the chamber from the previous exposure and which would react readily with the hydrogen-terminated sulfur surface. The slight increase in the methyl desorption signal with the number of bilayers thus simply reflects the fact that, with the larger number of dosing cycles, the cumulative wall exposure to DMCd increases.

The bottom spectra in Fig. 5 show desorption of $m/e^+ = 34$, i.e. H_2S. The measured desorption spectra for the lower mass ions, i.e. HS and S, were identical in shape and position to those for the parent ion as shown in Fig. 5, indicating that they originated from cracking of H_2S in the mass spectrometer. The desorption temperature of this feature was peaked at 480 K, irrespective of the number of bilayers. This desorbed H_2S is attributed to recombinative desorption of surface HS species, a process which removes the surface hydrogen and leaves about 0.5 monolayer of sulfur bonded to the surface metal layer (see the sketches in Fig. 6). This interpretation is supported by the fact that NEXAFS experiments show that, *after* H_2S exposure, surfaces containing integral numbers of bilayers are found to have both a strong sulfur L-edge feature corresponding to CdS and a feature attributed to SH. In addition, after heating this surface to more than 480 K, the SH feature was extinguished leaving only the features corresponding to CdS [15]. In comparison, other TPD studies of H_2S-dosed GaAs(100) [11] and transition metal (100) [17–19] surfaces have been reported in which chemisorbed H_2S dissociates into HS and H species. For GaAs(100), these SH and H species undergo recombinative desorption at 320 K; in addition, a process leading to dissociation of the remaining SH groups at 550 K, to produce adsorbed S and desorbed H, provides a second desorption channel. However, on heated Ni(100), Mo(100), and Rh(100), only the dissoci-

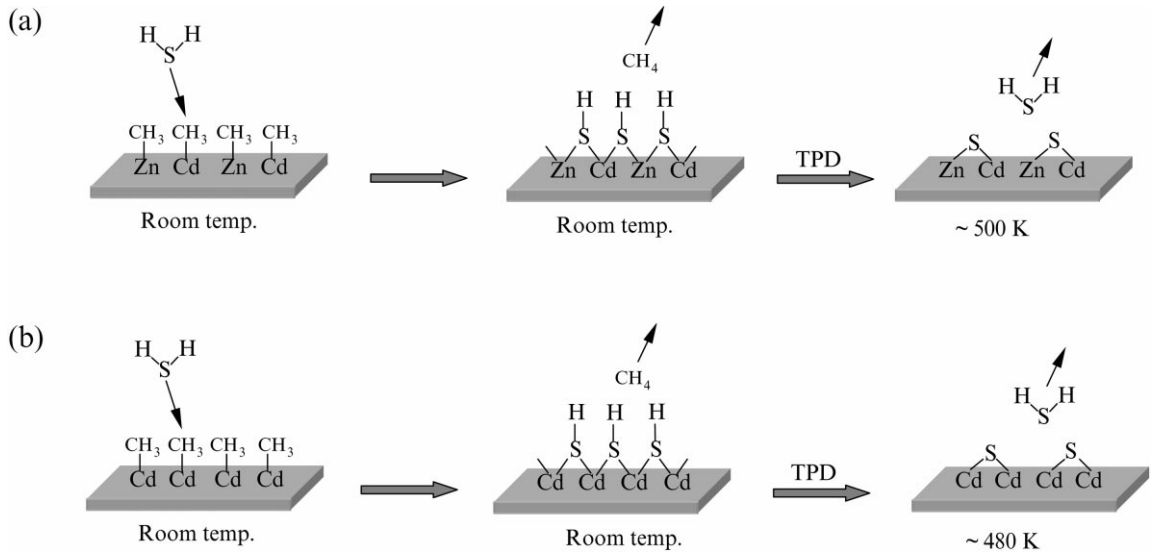

Fig. 6. Schematic depiction of surface chemistry for hydrogen-terminated surfaces. In all cases, only a recombinative desorption pathway is obtained. Panel (a) shows H_2S dosing of a methyl-terminated surface, formed by exposure of a bare ZnSe(100)-c(2×2) surface to DMCd and panel (b) shows H_2S dosing of a surface fully terminated with Cd–CH_3.

ation of HS species occurs, leaving stable sulfur-covered surfaces. This behavior is in accord with the fact that the transition metal–sulfur bond is much stronger than Ga–S, Zn–S and Cd–S bonds; most probably the transition metal chemistry involves empty d orbitals. In our case, as we will discuss later, on a fully HS-covered surface, recombinative desorption of H_2S is the only TPD channel.

Finally, note that the peak in the spectrum obtained from the 1.0 bilayer surface is asymmetric, suggesting heterogeneous SH bonding sites. This interpretation will be discussed in more detail in Section 3.2.2. Relatively symmetric peaks are seen, however, in the TPD spectra taken from the 2.0 and 4.0 bilayer surfaces, indicating that the bonding sites for HS species for these surfaces are homogeneous and that the reaction is predominantly of second order. The slight decrease in the peak area for H_2S ($m/e^+ = 34$) of the 4.0 bilayer surface is accompanied by a small increase in the peak area for CH_3 ($m/e^+ = 15$) on the same surface, suggesting that some S–H sites have reacted with trace amounts of DMCd in the chamber.

3.2. TPD measurements of the dose dependence of surface reactions in the first bilayer

It is of importance to understand the formation of the first bilayer for two reasons. First, the structure and composition of this layer determine the interfacial properties of this CdS–ZnSe heterosystem. Second, the properties of this layer also influence all subsequent chemisorption reactions. Note also that, unlike all subsequent bilayers, growth of the first layer involves a half-metallized substrate. In order to understand the detailed mechanism of the surface reaction in the first bilayer, a series of measurements were made of the surface concentration of CH_3 following exposure of ZnSe(100)-c(2×2) to DMCd. The TPD study also included measurements of the DMCd-dose dependence of the first bilayer reaction with a constant saturating dose of H_2S.

3.2.1. DMCd on ZnSe(100)-c(2×2)

The TPD spectra in this section were obtained following exposure of the c(2×2) surface to different doses of DMCd; the surface was either at liquid-nitrogen temperature ($\sim$100 K) or room temperature ($\sim$300 K). In each case, the TPD spectra showed the identical desorption peaks of DMZn at 372 K[1]. The equal intensity of the desorbed DMZn signals obtained from the substrate dosed at either $\sim$100 or 300 K implies that relatively strong DMCd chemisorption of a certain form must occur prior to the desorption of the physisorbed precursor, indicating this energy barrier for this chemisorption is very low[2].

The DMCd dose dependence of the detected methyl radical and MMZn signals is shown in Fig. 7a for a sample dosed at 300 K. The peak desorption temperature of both species was 370 K for the entire range of DMCd exposure shown in the figure. Since direct calibration of coverage was not possible, the relative intensities of desorption signals were used to measure the coverage of surface species as a function of DMCd exposure. Curves (1) and (2) display the peak heights of the TPD signals of the methyl radical and MMZn, respectively. Both curves show identical trends and both saturate at approximately the same value of DMCd exposure. However, as shown in Fig. 7b, the AES curve (2) for the surface Cd signal, also prepared at room temperature, does not exhibit the same behavior as curve (1) for the TPD signal of methyl radicals; in fact, the surface Cd concentration saturates at a higher value of DMCd exposure.

Specifically, as mentioned earlier, the desorbed DMZn signal provides a probe of the concentration of surface methyl groups for the first layer. Thus the curves in Fig. 7b show that the amount of surface Cd is still increasing even after the concentration of surface methyl groups has

[1] Note that for the substrate at about 100 K, there was also a desorption peak corresponding to physisorbed DMCd at 160 K.

[2] NEXAFS data demonstrated that, at 300 K and above, DMCd dissociatively chemisorbs on ZnSe(100)-c(2×2) surface. However, rigorously speaking, there are not enough data to give the low-temperature limit for the dissociation of DMCd on this surface, i.e. at what temperature methyl groups transfer to surface Zn atoms. Thus, we cannot rule out the possibility of the existence of a molecular chemisorption of one monolayer DMCd at temperatures below 300 K.

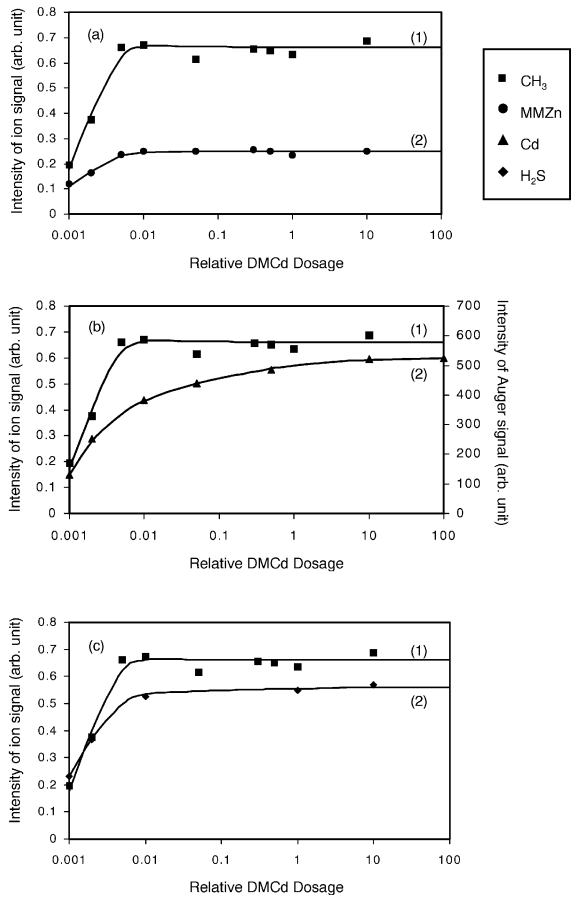

Fig. 7. TPD and Cd AES peak intensities versus the initial DMCd dosage on a ZnSe(100)-c(2×2) surface. (a) CH_3 ($m/e^+=15$) and MMZn ($m/e^+=79$) signals are shown as a function of DMCd dosage. (b) Surface Cd AES peak intensity is plotted together with the CH_3 ($m/e^+=15$) desorption signal. (c) Each point on curve (2) for H_2S desorption was obtained by dosing the surface to 100 relative exposure units of H_2S, following an initial, variable exposure to DMCd. Note that, as explained in the Section 2, the values of exposure shown here are relative; the actual exposure is about 3×10^3 times the relative values.

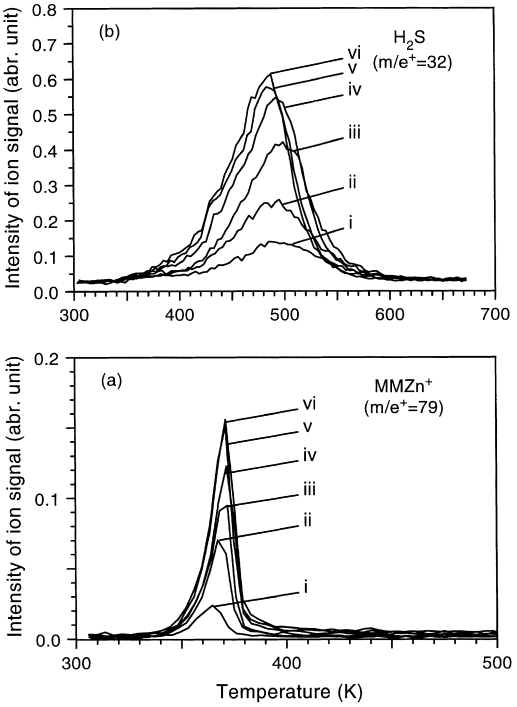

Fig. 8. Panel (a) shows a series of TPD curves of MMZn ($m/e^+=79$) obtained subsequent to exposing the ZnSe (100)-c(2×2) surface to (i) 0.0005, (ii) 0.001, (iii) 0.004, (iv) 0.02, (v) 0.2 and (vi) 10 relative exposure units (see text) of DMCd. Panel (b) shows H_2S ($m/e^+=34$) TPD curves obtained after first dosing the bare ZnSe surface with (i) 0.0005, (ii) 0.001, (iii) 0.002, (iv) 0.01, (v) 1 and (vi) 10 relative exposure units of DMCd followed by dosing with 100 relative exposure units of H_2S.

reached a constant saturated value. This behavior suggests the interplay of two reactions on the surface, namely a methyl-exchange reaction of DMCd with ZnSe(100), at low coverage, and a preferential replacement of Zn with Cd at high coverage. A detailed discussion of this interpretation is provided in Section 4.2.

Notice that, as shown in curve (2) in Fig. 7b, despite the fact that the Cd 'uptake' curve continues to increase, curve (2) in Fig. 7a for MMZn, which probes the desorption of DMZn, does not decrease even at high surface Cd coverage. Apparently, the substrate ZnSe, through diffusion from the bulk and into or through the surface Cd layer, provides an ample source of Zn to form DMZn and the formation of DMZn is limited only by the concentration of surface methyl groups.

Fig. 8a shows the TPD spectra obtained from the ZnSe surface after different DMCd exposures. As shown in the figure, the MMZn ($m/e^+=79$) feature has a single asymmetric peak with a relatively narrow full width at half-maximum (~15 K). A careful analysis shows that the peak

desorption temperature is almost independent of coverage, indicating a first-order reaction. First-order desorption would occur if two methyl groups are localized adjacent to a surface Zn before the desorption temperature is reached. This result suggests that surface methyl groups are energetically favored to exist as pairs even below saturation coverage. The narrow width of the desorption peaks is strong evidence that all the binding sites of the surface species are equivalent. Using Redhead's equation for first-order desorption [20] and a pre-exponential factor of $10^{13}\,s^{-1}$ gives an average activation energy of 22.8 kcal mol^{-1} for this desorption peak. A slight increase of peak temperature with increasing coverage, such as seen here, suggests a weakly attractive adsorbate interaction.

Although a complete understanding of this surface phenomenon requires a comprehensive investigation using different surface probes, e.g. STM, surface vibration spectroscopy, etc., based on current results, we can propose two possible schemes for the localization of methyl groups. In the first, adsorbed DMZn would already exist prior to its desorption, i.e. each Zn atom has two methyl bonded to it and remains molecularly adsorbed on the surface. However, since desorption of multilayer DMZn occurs at 160 K, it is difficult to explain how DMZn molecules can bond to the surface in a molecular form up to the known desorption temperature ($\sim$370 K). In the second scheme, Zn and Cd atoms remain on the surface in the form of monomethyl species. If, however, methyl groups have a tendency to pair up on top of the nearest neighboring Zn and Cd atoms, even at low coverage, this would require an attractive interaction associated with this configuration. Such a phenomenon has been seen, for example, in the desorption of H_2 from the Si(100)-2 × 1 monohydride state [21]; in this case hydrogen pairing at the Si dimers results in a first-order like desorption.

Additionally, experiments were made to detect Cd-related species ($m/e^+ = 112$, 127 and 142) at different DMCd exposures using TPD. No significant features were seen in these spectra except for a rising signal at $\sim$550 K for Cd $m/e^+ = 112$. This high-temperature Cd signal became sharper with increasing DMCd exposure. Prior observations on the surfaces of III–V crystals have shown that, after desorption of capping ligands, the surface structure became unstable, thus forming surface-supported metal droplets as the temperature increased [1,22]. However, in our study, we have found no evidence for the formation of Cd droplets. In particular, no significant decrease of Cd AES intensity was observed after the sample was heated to 620 K. In addition, in the TPD measurements, an elemental Cd signal did not appear until above 550 K; thus the activation energy for desorption of atomic Cd is much higher than the heat of vaporization of metallic cadmium (26.7 kcal mol^{-1}) [23]. It is reasonable therefore to consider that covalent bonded Cd remains on the surface and desorbs at high temperature by breaking Cd–Se or Cd–S bonds. Our temperature ramp did not reach the temperature of the Cd desorption peak and, thus, did not allow us to derive the desorption activation energy. However, our observations of high-temperature atomic Cd desorption do not preclude the existence of strong Cd–Se (46.8 kcal mol^{-1}) and Cd–S (48 kcal mol^{-1}) bonds [23]. Finally, note that Sides et al. also found the appearance of desorbed Cd at temperatures above 550 K corresponding to the sublimation of Cd atoms from the substrate CdTe(100) [12].

3.2.2. H_2S reactions with DMCd-exposed ZnSe(100)

To further understand the surface chemistry which occurs at the interface, TPD experiments were also performed on a surface formed with a variable exposure to DMCd followed by a saturated dose of H_2S. The experiments measured the dependence of the H_2S desorption signal on the value of the initial DMCd exposure. The peak intensity of the desorption signal for $m/e^+ = 34$ versus the initial DMCd dosage is shown in Fig. 7c. The measurements show that the desorbed H_2S tracks the surface methyl concentration in the first layer, see curve (1) in the same figure. The relative methyl concentration was obtained as described in the previous section. As discussed above, surface Cd and Zn concentrations vary as a function of the initial DMCd dose. The fact that the surface-sulfur coverage correlates only with the surface concentration of CH_3 but not of Cd or Zn is

consistent with H_2S reacting only with surface methyl groups on either Cd or Zn to form an HS-terminated surface.

Additionally, the signals from methyl radicals ($m/e^+ = 15$) were also measured *after* saturated H_2S dosing for different values of initial DMCd exposure. The results showed that, except for much greater exposures of DMCd than the saturating dose, there was no significant CH_3 signal after dosing H_2S. This result suggests that dosing with H_2S removes all surface methyl groups. Recall that the appearance of a trace concentration of methyl groups, following a high DMCd exposure, previously seen in Fig. 5, is attributed to the residual DMCd on the chamber walls which, after slowly desorbing, reacted with the HS species on the surface.

Finally, Fig. 8b shows TPD measurements of desorbed H_2S using the same dosing procedure as discussed in the previous two paragraphs. One clear qualitative feature of these curves is the decrease in peak temperature (500 K→483 K) with increasing initial DMCd dose. This peak-temperature decrease most probably results from a combination of two possible effects. First, since desorbed H_2S results from recombination of two surface HS species, the process is second order in surface coverage and, thus, the desorption peak shifts to lower temperature as terminal methyl groups and, hence, after reaction, the surface-HS concentrations increase. Alternatively, the shift in desorption temperature may also originate from the differences in bond energies between S–Cd and S–Zn. In particular, as shown in step 2 of Fig. 1, a surface-HS species can bond to either Zn or Cd. As mentioned below the Zn–S bond is stronger than the Cd–S bond. At low DMCd exposures, the concentration of surface Zn-methyl species is relatively high; this leads to the presence of a higher Zn–SH to Cd–SH ratio after H_2S dosing than that at higher DMCd exposure. Thus, in this case, the recombination of surface HS, which involves breaking of two metal–S back bonds, would then occur at higher temperatures for higher surface-zinc concentrations. However, at higher DMCd exposures and, hence, higher Cd–SH concentration than that of Zn–SH, the recombination of surface HS should occur at slightly lower temperature. The observation of a broad and slightly asymmetric peak for the H_2S signal, which suggests heterogeneous bonding sites for surface-HS species, supports the above discussion. In addition, this asymmetry was not observed for the H_2S desorption peaks from 2.0, 4.0 bilayer surface (Fig. 5) where SH groups bond homogeneously to Cd atoms.

4. Discussion

4.1. Desorption of surface methyl groups

The results given above suggest that the dominant desorption species is DMZn from the 0.5 bilayer surface but free methyl radicals or methane from the 1.5 bilayer (or a higher half-bilayer) methyl-terminated surface. Unfortunately, as mentioned in Section 2, it is not possible to use the cracking pattern of our mass spectrometer to distinguish whether the desorbing species in the latter case is a methyl radical or methane; thus thermodynamic arguments plus other experimental observations must be used to address this question. Chemically, the reaction and desorption channels of these surface-methyl groups depend on the nature of the bonds between the methyl group and the surface as well as the relative strength of the C–H bond (for reference, the C–H bond energy in CH_4 is about 104 kcal mol^{-1} [24]) within a surface methyl group. In general, there are limited dehydrogenation channels for surface methyl groups. Prior work has shown that methyl groups on semiconductor surfaces may lose hydrogen through direct hydrogen desorption or abstraction of hydrogen by a neighboring surface methyl group resulting in methane desorption. In an example of the first desorption channel, Rueter and Vohs [25] reported hydrogen desorption from methyl groups on Si (100) at about 850 K. In an example of the second channel, Rueter and Vohs in a separate study [16] described methyl desorption from GaAs(100) in the form of methane after hydrogen abstraction from an adjacent surface methyl at about 575 K. In addition, the authors also observed methyl *radical* desorption from the same

surface about 625 K. These observations of methyl dehydrogenation/dissociation at relatively high temperatures are in line with the strong C–H bonds of surface methyl groups on many semiconductor surfaces.

In contrast to these results on GaAs and Si surfaces, our work shows that surface methyl groups desorb from a Cd–CH_3-terminated II–VI surface before the characteristic temperature of dehydrogenation. This observation is consistent with the fact that CH_3 has a weaker bond to Cd (43.5 kcal mol^{-1} in DMCd) [26] than to Ga (59.5 kcal mol^{-1} in TMGa) [27] and much weaker when compared with CH_3–Si ($\sim$90 kcal mol^{-1}) [24]. Since in our case the growth surface is exposed to DMCd at a low, i.e. room temperature, it is unlikely that the dehydrogenation of the surface methyl groups will occur during the growth. On the other hand, during our TPD experiments higher surface temperatures are used and all detectable hydrocarbon species desorb at temperatures less than 450 K. Based on literature values on other semiconductor surfaces, this temperature is still relatively low for hydrogen abstraction from neighboring methyl groups. Combining the TPD measurement and our earlier NEXAFS study, which showed there is no unsaturated carbon species on the surface after a DMCd exposure, we conclude that the growth surface is terminated with methyl groups after dosing with DMCd and the surface methyl desorbs primarily either in the form of DMZn or methyl radical rather than methane (see Fig. 4). No surface dehydrogenation occurs during the low-temperature growth.

4.2. Surface methyl-exchange chemistry

Earlier we presented data showing that the surface methylation reaction changes in going from low to high DMCd exposure. In this section we discuss this change in more detail. The equations for the surface reactions may be written as:

$$Cd(CH_3)_{2(g)} \rightarrow Cd(CH_3)_{2(ads)}, \quad (1)$$

$$Cd(CH_3)_{2(ads)} + Zn_{(suf)} \rightarrow Cd(CH_3)_{(ads)} + Zn(CH_3)_{(ads)}, \quad (2)$$

$$Cd(CH_3)_{2(g)} + Zn(CH_3)_{(ads)} \rightarrow Cd(CH_3)_{(ads)} + Zn(CH_3)_2\uparrow, \quad (3)$$

$$Cd(CH_3)_{(ads)} + Zn(CH_3)_{(ads)} \rightarrow Cd_{(ads)} + Zn(CH_3)_{2(ads)}, \quad (4)$$

$$Zn(CH_3)_{2(ads)} \rightarrow Zn(CH_3)_2\uparrow. \quad (5)$$

These reactions show that at low DMCd exposure, surface methylation occurs by methyl exchange to Zn sites, i.e. reactions (1) and (2) dominate. The evolution of DMZn during the subsequent temperature ramp, i.e. reaction (4) with reaction (5), from such a surface is mostly through a Langmuir–Hinshelwood mechanism, i.e. abstraction of a surface methyl by an MMZn from a neighboring MMCd adsorbate. However, at high DMCd exposure, the concentration of surface methyl groups has already saturated and the replacement of Zn with Cd and subsequent desorption of DMZn, reaction (3), is the reaction pathway for DMCd. In this case, it is likely that DMCd reacts with an MMZn adsorbate and loses a CH_3 group to form DMZn; DMZn then desorbs and MMCd coordinates with the empty MMZn site. The Cd uptake curve (2) in Fig. 7b shows that this process reaches an asymptotic limit only at very high coverage, indicating the reaction precedes slowly, even at room temperature.

The observations in this paper show clearly the importance of methyl-exchange chemistry for desorption. Similar observations have been made by McCaulley and Donnelly for the adsorption of TMIn on GaAs(100) [28], which yielded desorbed TMGa after heating; and by Lasky, et al. for chemisorbed DMCd on GaAs (110) [29], which resulted in desorption of volatile TMGa. These observations suggest that the relative bond strengths of the lattice and adsorbate determine the reaction pathways, on both III–V and II–IV semiconductors. For the isolated molecule, breaking of the first CH_3–metal bond requires 43.5 and 47.2 kcal mol^{-1} for DMCd and DMZn, respectively, while the total energy required to remove all methyl groups is 65.6 and 82.9 kcal mol^{-1}, respectively [26]. Thus, since, the bond energies of bi-atomic ZnSe and CdSe are 32.6 and 46.8 kcal mol^{-1} [23], methyl exchange from Cd

to Zn should be exothermic by about 17.9 kcal mol^{-1}; hence DMZn desorption is the preferred demethylation route for a surface containing Zn and Cd atoms.

4.3. Mechanisms for reactions of H_2S with a CH_3-terminated surface

Unlike the case of GaAs(100) [10], our AES and TPD data show that a bare metal-terminated surface of a II–VI semiconductor does not react with H_2S. Instead, the formation of a sulfur-containing layer during growth is through methyl-aided chemisorption of H_2S, i.e. either through strong molecular adsorption of H_2S or reaction of H_2S with surface methyl groups. We can eliminate the possibility of molecular adsorption based on the fact that, in this case, methyl groups would remain on the surface, while, in fact, no detectable carbon was observed in either our AES or NEXAFS measurements after H_2S adsorption on a methyl-terminated surface [8,15]. In addition, these same NEXAFS measurements also detected the dissociation of H_2S after the chemisorption step. As a result, we only need to consider reactive chemisorption.

There are several possible reaction pathways for H_2S to react at room temperature with the methyl-terminated, group-II metal surface, including:

$$2(\mathrm{Cd{-}CH_3})_{(ads)} + \mathrm{H_2S_{(g)}} \rightarrow \mathrm{Cd{-}S{-}Cd_{(ads)}} + 2\mathrm{CH_4}\uparrow, \quad (6)$$

$$\mathrm{Cd{-}CH_{3(ads)}} + \mathrm{H_2S_{(g)}} \rightarrow \mathrm{Cd{-}H_{(ads)}} + \mathrm{CH_3SH}\uparrow \text{ or } \mathrm{CH_3SH_{(ads)}}, \quad (7)$$

$$\mathrm{Cd{-}CH_{3(ads)}} + \mathrm{H_2S_{(g)}} \rightarrow \mathrm{Cd{-}SH_{(ads)}} + \mathrm{CH_4}\uparrow. \quad (8)$$

For reaction (6), only one half of a monolayer of sulfur could be chemisorbed, and the relative stoichiometry for Cd to S of a thick film should be 2:1 for Cd to S. However, our earlier AES data on an epitaxial 15 bilayer sample [8] showed a Cd to S ratio of 1:1, as calibrated by the Auger intensity ratio measured on a bulk CdS crystal. Thus, the ratio of adsorbed precursor H_2S to surface Cd–CH_3 sites must be 1:1 for repetitive growth. In addition, our TPD data, presented above, showed that (only) H_2S desorbed, i.e. recombinatively, from a H_2S-exposed methyl-terminated surface, thus indicating that the reacted surface contained terminal hydrogen, prior to TPD measurements. These experimental results suggest that reaction (6) is not the dominant reaction channel.

Reactions (7) and (8) would both yield a 1:1 ratio of surface methyl to reacted molecular H_2S and leave hydrogen-containing surfaces after reactions. However, the desorption of surface methyl through formation of methane, i.e. reaction (8), is more energetically favorable than reaction (7). Specifically, both reactions (7) and (8) require that a surface Cd–CH_3 bond and a H–S bond from H_2S have to be broken. However, the energy gained in reaction (7) by forming a Cd–H bond ($\sim$16 kcal mol^{-1}) [23] and a CH_3SH bond ($\sim$74 kcal mol^{-1}) [24] is less than that in reaction (8), which forms Cd–SH ($\sim$48 kcal mol^{-1}) [23] and CH_3–H (104 kcal mol^{-1}) [24] bonds, and, thus on the basis of reaction energies and the known presence of SH, reaction (8) is the most reasonable reaction channel. These arguments are supported by our experimental measurements. In particular, if CH_3SH remained on the surface after reaction (7), AES, NEXAFS and TPD measurements would have detected carbon-related species, which is contrary to what has been observed in our measurements. Recall also that our experimental results using NEXAFS and TPD both showed that a sulfur-hydride-terminated surface is formed after H_2S chemisorption. Thus, reaction pathway (7) also can be ruled out.

Finally it is of interest to speculate on the transition states for the reaction of H_2S with the terminal methyl group. The transition state for forming the HS-terminated surface in reaction (8) may proceed by (a) abstraction of a surface methyl by one hydrogen from H_2S, to yield desorbed CH_4 and HS bonds to surface Cd; or by (b) direct attack of Cd by the sulfur end of H_2S, and coordination with H and CH_3, leading to the breaking of one Cd–CH_3 bond and one H–S bond, again yielding desorbed CH_4, forming a Cd–SH bond. For (a) the barrier to the first step would appear to be too high because the formation of methane requires breaking of two strong bonds,

i.e. Cd–CH_3 (43.5 kcal mol^{-1}) [26] and HS–H ($\sim$90 kcal mol^{-1}) [24], before the final sulfur-hydride-terminated surface is obtained. On the other hand, for (b) it might be expected that the coordinate interactions could lower the reaction barrier through bypassing any energetic intermediate states and thus facilitate this slightly exothermic reaction of about 5 kcal mol^{-1}. Thus, from the kinetic point of view, (b) is more likely the reaction pathway.

5. Conclusions and implications

In this paper, surface reaction studies are described which use TPD and AES to examine a binary surface reaction sequence for chemisorbing ordered layers of CdS on ZnSe(100). Two reaction mechanisms are proposed for adsorption of DMCd on this substrate at room temperature. One is a methyl-exchange reaction, which is the dominant reaction pathway before the vacancies of the $c(2\times2)$ surface are fully filled with Cd. The other reaction is Cd replacement of surface Zn, which becomes dominant after the surface is saturated with metal. Both of these reactions form a methyl-terminated surface. While DMZn is the major desorption product from this methyl-terminated surface, its narrow, asymmetric desorption peak does not shift as a function of DMCd dosage, indicating a first-order desorption process. H_2S reacts with such a methyl-terminated surface and forms a sulfur-hydride-terminated surface. Desorption of H_2S from this surface can occur by a recombinative reaction of surface HS species. The TPD results with different initial DMCd exposure reveal that desorption of H_2S is a second-order reaction, and that the layer composition is determined by the nature of reaction and the reaction kinetics. For growth layer coverage above 0.5 bilayer, desorption from the methyl-passivated surface appears to occur dominantly by desorption of free CH_3 groups. While hydrogen abstraction by a neighboring surface CH_3 group cannot be definitely ruled out, both the low desorption temperature and separate NEXAFS measurements suggest that the $m/e^+=15$ signals, in this case are from free methyl groups.

From the wider perspective of ordered organometallic growth, our study offers several important insights. First, at the most fundamental surface chemical level, the chemical approach to ordered reactions described in the introduction appears to 'work'. Thus the reaction sequence shown schematically in Fig. 1 operates by the two displacement reactions for all except the first adsorbed layer. The fact that such a scheme is effective means that thin films of ordered materials can be synthesized at temperatures other than those usually employed for thermally driven organometallic growth. In addition, our study of the surface chemistry suggests several new approaches to such chemically controlled growth, including the use of multiple substrate temperatures and layer-dependent variation in the amount and the composition of the dosed precursors. In fact such an investigation is currently under way in our laboratory. Finally, our studies of the chemistry in the first monolayer show that interfacial chemical abruptness is an important area in which chemical control is particularly demanding owing to the surface compositional heterogeneity of many common surface reconstructions and to the importance of interdiffusion across the interface.

Acknowledgement

We gratefully acknowledge the support of this work by the NSF through award #DMR-96-32456 and instrumentation support by the Department of Energy, contract no. DE-FG02-90ER14104.

References

[1] J.R. Creighton, Surf. Sci. 234 (1990) 287.
[2] M.A. Rueter, J.M. Vohs, Surf. Sci. 301 (1994) 165.
[3] V.M. Donnelly, J.A. McCaulley, Surf. Sci. 238 (1990) 34.
[4] T. Sontola, M. Simpson, Atomic Layer Epitaxy, Chapman and Hall, New York, 1990.
[5] M.Y. Jow, B.Y. Maa, T. Morishita, P.D. Dapkus, J. Electron. Mater. 24 (1) (1995) 25.
[6] S.M. George, A.W. Ott, J.W. Klaus, J. Phys. Chem. 100 (31) (1996) 13121.
[7] J.A. Yarmoff, D.K. Shuh, T.D. Durbin, C.W. Lo, D.A.

Lapiano-Smith, F.R. McFeely, F.J. Himpsel, J. Vac. Sci. Technol. A 10 (4) (1992) 2303.
[8] Y. Luo, D. Slater, M. Han, J.E. Moryl, R.M. Osgood Jr., J. Appl. Phys. 71 (26) (1997) 3799.
[9] Y. Luo, D. Slater, M. Han, J.E. Moryl, R.M. Osgood Jr., J.E. Chen, Langmuir 14 (1998) 1493.
[10] S. Conrad, D.R. Mullins, Q.S. Xin, X.Y. Zhu, Appl. Surf. Sci. 107 (1996) 145.
[11] J.S. Foord, E.T. FitzGerald, Surf. Sci. 306 (1994) 29.
[12] K. Yong, J.J. Reinoso, A.J. Gellman, P.J. Sides, J. Cryst. Growth 174 (1997) 708.
[13] C.H. Park, D.J. Chadi, J. Phys. Rev. B 49 (23) (1994) 16467.
[14] L. Seehofer, G. Falkenberg, R.L. Johnson, V.H. Etgens, S. Tatarenko, D. Brun, B. Daudin, Appl. Phys. Lett. 67 (12) (1995) 1680.
[15] M. Han, Y. Luo, J.E. Moryl, R.M. Osgood Jr., J.G. Chen, Surf. Sci. 415 (1998) 251.
[16] M.A. Rueter, J.M. Vohs, Surf. Sci. 268 (1992) 217.
[17] Y. Zhou, J.M. White, Surf. Sci. 183 (1987) 363.
[18] J.L. Gland, E.B. Kollin, F. Zaera, Langmuir 4 (1988) 118.
[19] R.I. Hegde, J.M. White, J. Phys. Chem. 90 (1986) 296.
[20] P.A. Redhead, Vacuum 12 (1962) 203.
[21] U. Höfer, Leping Li, T.F. Heinz, Phys. Rev. B 45 (16) (1992) 9485.
[22] J.A. McCaulley, V.M. Donnelly, J. Chem. Phys. 91 (1) (1989) 4330.
[23] CRC Handbook of Chemistry and Physics, CRC Press, Boca Raton, FL, 1985.
[24] D.F. McMillen, D.M. Golden, Annu. Rev. Phys. Chem. 33 (1982) 493.
[25] M.A. Rueter, J.M. Vohs, J. Vac. Sci. Technol. A 9 (6) (1991) 2916.
[26] L.H. Long, Pure. Appl. Chem. 2 (1961) 61.
[27] M.G. Jacko, S.J.W. Price, Can. J. Chem. 41 (1963) 1560.
[28] V.M. Donnelly, J.A. McCaulley, Surf. Sci. 235 (1990) L333.
[29] P.J. Lasky, P.H. Lu, Y. Luo, D.A. Slater, R.M. Osgood Jr., Surf. Sci. 364 (1996) 312.